Analytical approach to the Davydov-Scott theory with on-site potential

Yaroslav Zolotaryuk[1,2] and J. Chris Eilbeck[1]
[1]*Department of Mathematics, Heriot-Watt University, Edinburgh EH14 4AS, United Kingdom*
[2]*Max-Planck-Institut für Physik komplexer Systeme, Nöthnitzer Strasse 38, D-01187 Dresden, Germany*
(Received 11 August 2000; published 11 January 2001)

We propose an analytical approach to study the one-dimensional acoustic polaron model that includes an on-site external potential applied to each chain molecule. The key to the approach is an exact discrete solution for the chain-deformation field given in terms of a (quasi)particle wave function. For this purpose we introduce a set of polynomial series that resemble the Chebyshev polynomials. We call these series the hyperbolic Chebyshev polynomials. Using next a properly chosen discrete trial function for the wave function envelope, we obtain simple expressions for the variational energy of the system. Contrary to an isolated (without any external potential) molecular chain, the polaron state (Davydov soliton) is shown to exist only for appropriate system parameters while the delocalized (exciton) state can always exist. As a result, the following three regimes can be specified for the chain with an on-site potential: (i) the polaron is a ground state and the exciton is a metastable state, (ii) the polaron is a metastable state and the exciton is a (delocalized) ground state, and (iii) the polaron state does not exist and only the exciton exists, being a ground state. Two characteristic dimensionless parameters are found in terms of which a criterion of existence of (stable and metastable) polaron states and their nonexistence is formulated. Finally, the Davydov soliton experiences depinning in a particular case of system parameters, resulting in a transparent regime of uniform propagation of the soliton with very small size.

DOI: 10.1103/PhysRevB.63.054302 PACS number(s): 63.20.Kr, 63.20.Ry, 63.20.Pw

I. INTRODUCTION

There has been renewed interest in the Davydov soliton and polarons in molecular chains[1,2] demonstrated by recent publications,[3–17] which have called into question different aspects of polaron dynamics and self-trapping. Historically, one-dimensional polaron models received a major impetus from the work of Davydov and Kislukha,[18] who used the exciton formalism to describe the steady-state propagation of a self-localized intramolecular excitation (generally, a quantum particle) along a molecular (polypeptide) chain. This transfer process, often referred to as the Davydov-Scott self-trapping mechanism of energy transfer in protein, involves high-frequency intramolecular motions (considered by Takeno[19] as classical oscillators) that are coupled to low-frequency acoustic (as in the original Davydov model[1–3,7–10,18,20]) or optical (as in the Holstein model[4,6,11–15,21–23]) phonon motions.

The purpose of the present paper is to investigate the problem of existence of self-localized (polaron) states in a molecular chain interacting with its environment, contrary to the original acoustic Davydov model in which the chain of coupled massive molecules is considered as an isolated object. Thus, each hydrogen-bonded molecular chain in the α-helix protein or in crystalline acetanilide[22,23] is tightly coupled to a three-dimensional complex skeleton and therefore each molecule of the chain has an equilibrium position given externally. The simplest way to describe the interaction of the molecular chain with such an atomic or molecular periodic environment is to introduce in the acoustic Davydov Hamiltonian a sequence of harmonic on-site potentials and to place each chain molecule in this potential, allowing it to vibrate with low frequency around the potential bottom.[17,24,25] Thus, our generalized polaron Hamiltonian consists of three parts:

$$\hat{H}=\hat{H}_{\rm qp}+\hat{H}_{\rm ph}+\hat{H}_{\rm qp\text{-}ph} \tag{1}$$

where $\hat{H}_{\rm qp}$ describes a single free quantum particle or quasiparticle (an exciton or an extra electron) in the chain, $\hat{H}_{\rm ph}$ is the phonon Hamiltonian, and $\hat{H}_{\rm qp\text{-}ph}$ describes the interaction of the quantum (quasi)particle with acoustic phonons of the chain.

The first term in the right-hand side of Eq. (1) is the usual tight-binding Hamiltonian for a quantum (quasi)particle,

$$\hat{H}_{\rm qp}=\sum_n\ [\mathcal{E}_0 a_n^\dagger a_n - J(a_n^\dagger a_{n+1}+a_{n+1}^\dagger a_n)], \tag{2}$$

where $\mathcal{E}_0$ is the (quasi)particle energy in the undistorted chain, J the hopping amplitude (e.g., the dipole-dipole interaction strength between intramolecular vibrations, when the chain is undistorted), and $a_n^\dagger(a_n)$ are the Bose or Fermi creation (annihilation) operators of the (quasi)particle associated with the nth molecule of the chain.

The second part of Eq. (1) describes the phonon displacement field $\hat{Q}_n$ interacting (in the harmonic approximation) with a periodic substrate potential, so that each chain molecule is assumed to be influenced by the local harmonic potential with a force constant κ_0:

$$\hat{H}_{\rm ph}=\sum_n\ \left[\frac{\hat{P}_n^2}{2M}+\frac{K}{2}(\hat{Q}_{n+1}-\hat{Q}_n)^2+\frac{\kappa_0}{2}\hat{Q}_n^2\right]. \tag{3}$$

Here M is the molecular mass, K is the force constant of the interaction between molecules, and the lattice field operators

$\hat{P}_n$ and $\hat{Q}_n$ are the momentum and displacement from the equilibrium position of the nth chain molecule.

The third part of the Hamiltonian $\hat{H}$ describes the (quasi)particle-phonon interaction that consists of two portions.[20] One of these appears under the assumption that (quasi)particle band energy depends linearly on the distance between the nearest-neighbor molecules as $\mathcal{E}_n=\mathcal{E}_0+\chi_1(Q_{n+1}-Q_{n-1})$, whereas the appearance of the other interaction term is associated with the linear dependence of the amplitude of hopping between the nth and $(n+1)$th molecules: $J_{n,n+1}=J-\chi_2(Q_{n+1}-Q_n)$, meaning that the hopping amplitude decreases with increase of the distance between the adjacent molecules. Thus, the Hamiltonian that describes such a combined (quasi)particle-interaction and was also introduced in earlier studies[20,26] reads

$$\hat{H}_{\text{qp-ph}}=\chi_1\sum_n a_n^\dagger a_n(\hat{Q}_{n+1}-\hat{Q}_{n-1}) + \chi_2\sum_n (a_n^\dagger a_{n+1}+a_{n+1}^\dagger a_n)(\hat{Q}_{n+1}-\hat{Q}_n). \quad (4)$$

Using the adiabatic Davydov ansatz[1,2] with the corresponding techniques,[27] one finds that the Hamiltonian (1)–(4) results in the following system of two coupled classical equations of motion:

$$i\hbar\dot{\psi}_n=\mathcal{E}_0\psi_n-J(\psi_{n-1}+\psi_{n+1})+\chi_1(Q_{n+1}-Q_{n-1})\psi_n + \chi_2[(Q_n-Q_{n-1})\psi_{n-1}+(Q_{n+1}-Q_n)\psi_{n+1}], \quad (5)$$

$$\ddot{Q}_n=K(Q_{n+1}-2Q_n+Q_{n-1})-\kappa_0 Q_n+\chi_1(|\psi_{n+1}|^2 - |\psi_{n-1}|^2)+2\chi_2\,\mathrm{Re}[\psi_n^*(\psi_{n+1}-\psi_{n-1})], \quad (6)$$

where $\psi_n(t)$ is the discrete complex-valued wave function of the (quasi)particle and $Q_n(t)$ is the classical lattice field of the molecule's displacements from their equilibrium positions, $n=0,\pm1,\ldots$. These equations are complemented by the normalization condition $\Sigma_n|\psi_n(t)|^2=1$.

In the particular case when the phonon term with the on-site oscillators is absent ($\kappa_0=0$), Eqs. (5) and (6) reduce to the usual Davydov model.[1,2] In this case, each of the (quasi)particle-phonon coupling constants χ_1 or χ_2 results in the existence of self-localized states for all values of the system parameters. Moreover, Eqs. (5) and (6) are easily solved in the continuum limit and the self-trapping occurs with the additive coupling constant $\chi=\chi_1+\chi_2$. Therefore, the interaction term with χ_2 was rarely considered in literature. However, the situation in the discrete case appears to be more sophisticated because the physical origin of the constants χ_1 and χ_2 is different: the interaction with χ_1 is a result of lowering the on-site energy $\mathcal{E}_n$ under a chain compression, whereas the second (χ_2) interaction originates from increase of the hopping amplitude $J_{n,n+1}$ with this compression. Therefore, it is not clear what happens to a small (narrow) Davydov soliton when both these interactions are present in the theory. The present paper also aims to investigate how the interplay between the constants χ_1 and χ_2 results in mobility of the Davydov soliton.

On the other hand, the Hamiltonian (1)–(4) may also be referred to as the Holstein model[21] with a positive (because $K>0$) dispersion and a nonlocal electron-phonon coupling (with the two constants $\chi_1\geqslant0$ and $\chi_2\geqslant0$). We consider the following arguments. In the limiting case $K\to0$, when the coupling between the on-site oscillators is absent (it occurs only via the nonlocal electron-phonon coupling), it is not known whether polaron solutions exist. Indeed, in the continuum limit (when the site n is substituted by the spatial variable x), for the standing continuum envelope $\varphi(x)$ of the wave function $\psi_n(t)$, one can derive from Eqs. (5) and (6) the nonlinear Schrödinger equation with the nonlinearity $(\varphi^2)''\varphi$ (where the prime denotes the differentiation over x) that can easily be integrated and analyzed using phase-portrait techniques. As a result, this equation appears not to support solutions of the standard (bell-shaped) type that would correspond to self-localized states.

However, if we consider the discrete version of this model, using a variational approach (used in the present paper) to find the envelope φ_n in the form of a discrete trial function with exponential spatial decay, we find that, contrary to the continuum limit, the total energy of the system attains a minimum, but only if the constant $\chi_1^2/J\kappa_0$ exceeds a certain critical value. This means that there exists some critical value for the eigenfrequency of the on-site oscillators, above which the self-trapping effect disappears. The phonon dispersion should effectively soften this frequency so that the critical value will increase. This is why for the Davydov model with an on-site potential, the existence of self-localized states in some cases was numerically observed, but in other cases only delocalized states were obtained.[24] All these arguments demonstrate that the problem of the existence of self-localized states in the polaron model given by the Hamiltonian (1)–(4) is far from being fully understood.

The results in the present paper are obtained in two steps. First, we develop analytical techniques of summation of the whole variety of series using an algebra that is similar to that of the Chebyshev polynomials. This allows us to obtain all equations expressed only in terms of the envelope φ_n. Second, having in the theory only one lattice field φ_n, we are able to apply a simple variational approach using only *one* variational parameter. In this way, it is proved that final equations can be analyzed analytically. Particularly, a criterion for the existence of self-localized (both stable and metastable) states is obtained.

This paper is organized as follows. In the next section, we present the reduced equations of motion that are basic equations to be studied throughout this paper. In Sec. III, using the Chebyshev-like polynomials, we develop a procedure that gives an analytical solution for the lattice displacement field as a function of the wave-function envelope. In the next section, we apply a discrete variational approach to find this envelope by minimization. A criterion given as an implicit function of two dimensionless characteristic parameters is derived in Sec. V. The binding energy of the localized (quasi)particle is discussed in Sec. VI. This section also confirms a high accuracy of our variational approach. In Sec. VII, we

estimate the Peierls-Nabarro barrier for the self-localized states and find the particular case when polarons are depinned. Section VIII contains our conclusions. Finally, some results of analytical calculations are presented in Appendixes A and B.

II. REDUCED EQUATIONS TO BE STUDIED

For the dimensionless description we introduce scaled time $\tau = v_0 t/l$, where l is the lattice spacing and $v_0 = \sqrt{K/M}\,l$ is the sound velocity in the lattice subsystem. In terms of space and time-scaling parameters, both the (quasi-)particle wave function $\psi_n(t)$ and the displacement field $Q_n(t)$ can be rewritten as $\phi_n(\tau) = \exp[i(E_0 - 2J)t/\hbar]\psi_n(t)$ and $u_n(\tau) = Q_n(t)/l$. Next, we use the representation of the wave function $\phi_n(\tau)$ in the form of a modulated plane wave:

$$\phi_n(\tau) = \varphi_n(\tau)\exp\{i[nk - \sigma(\varepsilon_0 + \varepsilon)\tau]\} \tag{7}$$

where the characteristic parameter $\sigma = Jl/\hbar v_0$ measures the ratio of amplitudes for transfers from site to site in the (quasi)particle and phonon subsystems. Thus, for α-helix protein, the values $J = 7.8\ \mathrm{cm}^{-1}$ and $l = 4.5$ Å are known,[20] so that for velocities $v_0 \sim 10^3$ m/s one obtains $\sigma \sim 1$. The dimensionless energy $\varepsilon_0 = 2(1 - \cos k)$ describes the linear band spectrum of the linearized equation (5) and ε is the binding energy of the (quasi)particle to the chain. Using the representation (7) in Eqs. (5) and (6) and equating the real and imaginary parts of Eq. (5), we find the following three discrete equations:

$$\begin{aligned}\varepsilon\varphi_n = &-\cos k(\varphi_{n+1} - 2\varphi_n + \varphi_{n-1}) + (\alpha/2)\{(1-\eta)\\ &\times(u_{n+1} - u_{n-1})\varphi_n\\ &+ \eta\cos k[(u_n - u_{n-1})\varphi_{n-1}\\ &+ (u_{n+1} - u_n)\varphi_{n+1}]\},\end{aligned} \tag{8}$$

$$\begin{aligned}\frac{d\varphi_n}{d\tau} = &\sin k\{\sigma(\varphi_{n-1} - \varphi_{n+1}) + (\alpha\eta/2)[(u_{n+1} - u_n)\varphi_{n+1}\\ &- (u_n - u_{n-1})\varphi_{n-1}]\},\end{aligned} \tag{9}$$

$$\begin{aligned}\frac{d^2u_n}{d\tau^2} = &-(u_{n+1} - 2u_n + u_{n-1}) - \omega_0^2 u_n + \beta[(1-\eta)\\ &\times(\varphi_{n+1}^2 - \varphi_{n-1}^2)/2 + \eta\cos k\varphi_n(\varphi_{n+1} - \varphi_{n-1})].\end{aligned} \tag{10}$$

In these equations, the coupling constants χ_1 and χ_2 are redefined to the dimensionless quantities α and β according to the relations $\alpha = 2l(\chi_1 + \chi_2)/J$ and $\beta = 2l(\chi_1 + \chi_2)/Mv_0^2$.[25] We have also incorporated the partition parameter $\eta = \chi_2/(\chi_1 + \chi_2)$, $0 \leqslant \eta \leqslant 1$, so that $\eta = 0$ if $\chi_2 = 0$ and $\eta = 1$ if $\chi_1 = 0$.[26] The dimensionless frequency $\omega_0 = \sqrt{\kappa_0/K}$ measures the relative strength of the intermolecular and on-site interactions. Note that the former interactions effectively reduce the eigenfrequency of the on-site oscillators. Finally, the envelope $\varphi_n(\tau)$ satisfies the normalization condition

$$\sum_n \varphi_n^2 = 1. \tag{11}$$

The reduced equations (8)–(11) are the key objects to be studied in the present paper. As regards the spectral parameter ε in Eq. (8), it can be expressed in terms of the lattice fields φ_n and u_n as follows. Multiplying both sides of Eq. (8) by φ_n and summing them over n, and then using the normalization condition (11), we find

$$\begin{aligned}\varepsilon = &\cos k\sum_n (\varphi_{n+1} - \varphi_n)^2 + \frac{1}{2}\alpha\sum_n (1-\eta)(u_{n+1} - u_{n-1})\varphi_n\\ &+ \frac{1}{2}\alpha\eta\cos k[(u_n - u_{n-1})\varphi_{n-1} + (u_{n+1} - u_n)\varphi_{n+1}].\end{aligned} \tag{12}$$

In this paper we are interested only in traveling wave (TW) solutions of Eqs. (8)–(11). For this class of solutions one can write $\varphi_n(\tau) = \varphi(n - s\tau)$ and $u_n(\tau) = u(n - s\tau)$ where $s = v/v_0$ is the dimensionless propagation velocity. In the continuum limit, Eq. (9) is transformed to the relation between the wave number k and the velocity of wave propagation s,

$$s = 2\sigma\sin k. \tag{13}$$

Note that in the particular case of standing solutions ($s = 0$), Eq. (9) simply vanishes ($k = 0$). As for Eq. (10), in the continuum limit (again for TW solutions) one can approximately substitute the time derivative by the discrete time derivative: $d^2u_n/d\tau^2 \simeq s^2(u_{n+1} - 2u_n + u_{n-1})$. Then this equation can be rewritten concisely as

$$u_{n+1} - 2\zeta u_n + u_{n-1} = R_n \tag{14}$$

with the source term

$$R_n = G(1-\eta)(\varphi_{n-1}^2 - \varphi_{n+1}^2) + 2G\eta\cos k\varphi_n(\varphi_{n-1} - \varphi_{n+1}). \tag{15}$$

Here the constants ζ and G are defined by $\zeta = 1 + \omega_0^2/2(1 - s^2)$ and $G = \beta/2(1 - s^2)$. Therefore, Eq. (14) is appropriate for moving ($s > 0$) solutions if they are sufficiently smooth from site to site, but it also appears as an exact *discrete* equation for standing ($k = 0$ and $s = 0$) solutions.

As mentioned in the previous section, in the limiting case when the on-site potential disappears ($\omega_0 \to 0$ or $\zeta \to 1$), the system of Eqs. (8) and (14) is reduced to the usual acoustic polaron model.[1,2] In this particular case, the difference $u_{n+1} - u_n$ can easily be found from Eqs. (14) and (15) as a function of φ_n and φ_{n+1}. Inserting this function into Eq. (8), we obtain a stationary discrete nonlinear Schrödinger (DNLS) equation with cubic nonlinearity, the normalized solution of which in the continuum limit is well known: $\varphi_n(\tau) = \sqrt{\lambda/2}\,\mathrm{sech}[\lambda(n - s\tau)]$, and $\varepsilon = -\lambda^2\cos k$ with the reduced coupling constant

$$\lambda = \alpha\beta(1 - \eta + \eta\cos k)^2/4(1 - s^2)\cos k. \tag{16}$$

For instance, in the case of α-helix protein, the mass of a peptide group is $M=114m_p$, where m_p is the proton mass and the coupling constant was estimated as $\chi_1=3.4\times10^{-11}$ N. Therefore, the constant λ at $k=0$ is of order ten. Also note that for $k=0$, the constant λ does not depend on the partition parameter η because both the constants χ_1 and χ_2 are present in the theory additively. As can be seen from this solution, the constant λ is a characteristic parameter of the theory, since it determines the soliton size and the energy level ε.

III. DECOUPLING PROCEDURE AND HYPERBOLIC CHEBYSHEV POLYNOMIALS

In a general case when $\zeta>1$, we cannot express so easily the difference $u_{n+1}-u_n$ through the envelope φ_n as in the limiting case $\zeta\to1$. But this step is necessary in order to get a nonlinear Schrödinger equation given in terms of only φ_n. In this section, using the explicit representation of Chebyshev-like polynomials, we develop a procedure that allows us to solve this problem. This is the most important point of our findings. In this way we are able to decouple the lattice fields φ_n and u_n and we call this scheme a decoupling procedure.

Let us consider the solutions of the two types of symmetry: the center of the φ_n profile is assumed to be localized at a lattice site (we call it a site-centered or S state) and the φ_n profile is centered in the middle of adjacent lattice sites (call it a bond-centered or B state). Next, let us suppose the φ_n profile to be centered at the site with $n=0$. Then one can write $\varphi_{-n}=\varphi_n$ $(n=0,\pm1,\dots)$. In the other case, assuming that the φ_n profile is centered in the middle between the sites with $n=0$ and $n=1$, we have $\varphi_{-n}=\varphi_{n+1}$ $(n=0,\pm1,\dots)$. Using these symmetry definitions in Eq. (15), we find that $R_{-n}=-R_n$ and $R_{-n}=-R_{n+1}$, $n=0,\pm1,\dots$, for the site- and bond-centered profiles, respectively. Using the last relations, one finds from Eq. (14) the symmetry properties of the displacement field u_n. Thus, the S and B symmetry properties can be summarized as follows:

$$\varphi_{-n}=\varphi_n,\quad u_{-n}=-u_n,\quad R_{-n}=-R_n, \tag{17}$$

for S symmetry and

$$\varphi_{-n}=\varphi_{n+1},\quad u_{-n}=-u_{n+1},\quad R_{-n}=-R_{n+1}, \tag{18}$$

for B symmetry, where $n=0,\pm1,\dots$. Below we treat self-localized states of both symmetries separately.

A. Site-centered self-localized states

In the case of solutions centered at the site with $n=0$, we have the identities $R_0=0$ and $u_0=0$, which immediately follow from the symmetry relations (17). Next, by induction, one can prove that the solution of the linear difference equation (14) can be represented in the form

$$u_n=K_{n-1}^{[2\zeta]}u_1+\sum_{j=1}^{n-1}K_{n-1-j}^{[2\zeta]}R_j,\quad n=2,3,\dots, \tag{19}$$

where $K_n^{[2\zeta]}=K_n^{[2\zeta]}(\zeta)$ is the Green's function defined by the recurrence formula

$$K_{n+2}^{[f(\zeta)]}(\zeta)=2\zeta K_{n+1}^{[f(\zeta)]}(\zeta)-K_n^{[f(\zeta)]}(\zeta),$$

$$K_0^{[f(\zeta)]}(\zeta)=1,\quad K_1^{[f(\zeta)]}(\zeta)=f(\zeta), \tag{20}$$

with the generating function $f(\zeta)$ indicated in the square brackets superscript. It is important that in the particular case when the generating function is $f(\zeta)=\zeta$, $1\leqslant\zeta<\infty$, the functions $K_n^{[f(\zeta)]}$ can be calculated explicitly:

$$K_n^{[\zeta]}(\zeta)\equiv T_n(\zeta)=\cosh(n\ \mathrm{Arcosh}\,\zeta)=(b^n+b^{-n})/2,$$

$$b=\zeta+\sqrt{\zeta^2-1}, \tag{21}$$

for all integers $n=0,1,\dots$. Since the algebra of these is ''hyperbolic,'' contrary to the usual Chebyshev polynomials defined in the interval $0\leqslant\zeta\leqslant1$, we call the set of functions (21) the *hyperbolic* Chebyshev polynomials.[28]

The next important step is that the $K_n^{[2\zeta]}$ polynomials, including also those with other generating functions $f(\zeta)$, can be expressed explicitly in terms of the polynomials $T_n(\zeta)$. Indeed, by induction, one can establish the identity

$$K_n^{[2\zeta]}-K_{n-2}^{[2\zeta]}=2T_n,\quad n=2,3,\dots. \tag{22}$$

Using this identity, we find separately for even and odd subscripts, the relations that allow us to write the functions $K_n^{(2\zeta)}$ through the polynomials T_n:

$$K_{2m}^{[2\zeta]}=1+2\sum_{j=1}^{m}T_{2j},\quad m=1,2,\dots;$$

$$K_{2m+1}^{[2\zeta]}=2\sum_{j=0}^{m}T_{2j+1},\quad m=0,1,\dots. \tag{23}$$

Finally, using the representation (23) and the explicit formula (21), one finds the explicit expression for the polynomials $K_n^{[2\zeta]}$:

$$K_n^{[2\zeta]}=\frac{b^{n+1}-b^{-n-1}}{b-b^{-1}},\quad n=0,1,\dots. \tag{24}$$

Now we need to calculate the displacement u_1 in Eq. (19). To this end, we use a boundary condition at the right end of the chain. Particularly, using the zero boundary condition $(\lim_{n\to\infty}u_n=0)$, we find from Eq. (19)

$$u_1=-\lim_{n\to\infty}\sum_{j=1}^{n-1}[K_{n-1-j}^{[2\zeta]}/K_{n-1}^{[2\zeta]}]R_j$$

$$=-\lim_{n\to\infty}\sum_{j=1}^{n-1}\frac{b^{n-j}-b^{-n+j}}{b^n-b^{-n}}R_j=-\sum_{j=1}^{\infty}b^{-j}R_j. \tag{25}$$

Thus, Eqs. (19), (24), and (25) determine the displacement field u_n, $n=1,2,\dots$, as a function of the envelope φ_n for each $\zeta>1$. Calculating next the relative displacements $u_{n+1}-u_n$ in terms of φ_n and substituting the resulting ex-

pressions in Eq. (8), we obtain a stationary DNLS equation. In the two particular cases $\eta=0$ ($\chi_2=0$) and $\eta=1$ ($\chi_1=0$), this equation is derived in Appendix A [see Eqs. (A4) and (A9)].

B. Bond-centered self-localized states

In the case of solutions centered in the middle between the sites with $n=0$ and $n=1$, the symmetry properties are determined by Eqs. (18). Using the equation $u_0=-u_1$, by induction, one can prove that the solution of the linear difference equation (14) is represented in the form

$$u_n=K_{n-1}^{[2\zeta+1]}u_1+\sum_{j=1}^{n-1}K_{n-1-j}^{[2\zeta]}R_j,\quad n=2,3,\ldots, \tag{26}$$

where the polynomials $K_n^{[2\zeta+1]}$ can also be expressed in terms of the hyperbolic Chebyshev polynomials T_n. Similarly, by induction, one can establish the identity

$$K_n^{[2\zeta+1]}(\zeta)=K_{n-1}^{[2\zeta]}(\zeta)+K_n^{[2\zeta]}(\zeta),\quad n=1,2,\ldots. \tag{27}$$

Using this equation and the representation (24), we find the explicit expression for the polynomials $K_n^{[2\zeta+1]}$,

$$K_n^{[2\zeta+1]}=\frac{b^{n+1}-b^{-n}}{b-1},\quad n=0,1,\ldots. \tag{28}$$

In the same way as for the *S* profiles, the displacement u_1 can be calculated, using the zero boundary condition at the right end of the chain. As a result, from Eq. (26) we find

$$\begin{aligned}u_1&=-\lim_{n\to\infty}\sum_{j=1}^{n-1}[K_{n-1-j}^{[2\zeta]}/K_{n-1}^{[2\zeta+1]}]R_j\\&=-\lim_{n\to\infty}\sum_{j=1}^{n-1}\frac{b^{n-j}-b^{-n+j}}{(b+1)(b^{n-1}-b^{-n})}R_j\\&=-\frac{1}{1+b^{-1}}\sum_{j=1}^{\infty}b^{-j}R_j.\end{aligned} \tag{29}$$

The corresponding DNLS equations are given by Eqs. (A14) and (A18).

IV. CALCULATION OF SELF-LOCALIZED STATES

When $\omega_0\neq 0$ ($b>1$), each of the stationary DNLS equations (A4), (A9), (A14), or (A18) cannot be solved analytically, because even in the continuum limit it becomes an integro-differential equation. Therefore, an appropriate variational method should be applied. From this point of view, the exact representations for the lattice displacement field u_n given by the series (A2), (A7), (A12), and (A16) with the corresponding coefficients A_{jn}, B_{jn}, C_{jn}, and D_{jn} [see Eqs. (A3), (A8), (13), and (A17)] appear to be very useful because they allow us to reduce significantly the number of variational parameters. We use a discrete trial function with only *one* variational parameter describing the size of self-localization. As a result, the polaron profiles and energy are found in a simple form.

First, we notice that the basic equations (8) and (14) can be represented as a minimum condition for the discrete energy functional $E(\{\varphi_n\},\{u_n\})$, written through the reduced Lagrangian function L:

$$\begin{aligned}E=-L=\cos k\sum_n\,&[(\varphi_{n+1}-\varphi_n)^2+(\alpha/2G\cos k)u_n\\&\times(R_n+\zeta u_n-u_{n+1})],\\&\zeta=(b+b^{-1})/2,\end{aligned} \tag{30}$$

where the constant term with ε has been omitted. This functional can also be obtained in the standard manner [as for the equations of motion (5) and (6)] from the Hamiltonian (1)–(4), using the same assumptions and notation that led to Eqs. (8) and (14). Inserting the representation for u_n given by Eqs. (A2), (A7), (A12), and (A16) in Eq. (30), we get the functional of *one* lattice field, i.e., $E(\{\varphi_n\})$. Therefore, a properly chosen discrete trial function with only one variational parameter can be used and its optimal value can be calculated analytically by minimization of the variational energy (30). Below we will apply this variational approach separately to the *S* and *B* polaron states.

A. Site-centered self-localized states

Thus, for the *S* polaron states, the trial function that describes the normalized [see Eq. (11)] envelope profile φ_n can be chosen in the form

$$\varphi_n=\sqrt{\frac{1-q^2}{1+q^2}}q^n,\quad n=0,\pm 1,\ldots. \tag{31}$$

Then, according to Eqs. (A2) and (A7), we find by straightforward calculation that the displacement field u_n is given by $u_0=0$ and

$$u_n=\frac{b(1-q^2)^2(q^{2n}-b^{-n})}{(1-bq^2)(b-q^2)}G \tag{32}$$

if $\eta=0$ and

$$u_n=\frac{2bq(1-q^2)^2(q^{2n}-b^{-n})}{(1+q^2)(1-bq^2)(b-q^2)}G\cos k, \tag{33}$$

if $\eta=1$, where $n=1,2,\ldots$. Inserting next the expressions (31)–(33) in the functional (30) and using the symmetry properties of the lattice fields φ_n and u_n [see Eq. (17)] as well as the definitions (15), (A5), and (A10), by direct but lengthy calculations we obtain

$$\frac{E_{S\nu}(b,\lambda_\nu;q)}{\cos k}=2\frac{(1-q)^2}{1+q^2}-\lambda_\nu\frac{(1-q^2)^3}{(b-q^2)^2}P_{S\nu}(b;q),\quad \nu=0,1, \tag{34}$$

where the subscript $\nu=0$ ($\nu=1$) corresponds to the case $\eta=0$ ($\eta=1$) and the functions $P_{S\nu}(b;q)$ are presented in Appendix B [see Eq. (B1)]. Note that both the functions $P_{S\nu}$ have small variation in the interval $0\leqslant q\leqslant 1$ and tend to $b/2$ when $q\to 1$.

B. Bond-centered self-localized states

For the *B* polaron states the trial function for the envelope φ_n can be chosen in the form

$$\varphi_n = \sqrt{\frac{1-q^2}{2}}\, q^{n-1}, \quad n=1,2,\ldots . \tag{35}$$

Similarly, according to Eqs. (A12), (A13), (A16), and (A17), we find

$$u_n = \frac{b(1-q^2)^2[(1+q^{-2})q^{2n}-(b+1)b^{-n}]}{2(1-bq^2)(b-q^2)}G, \tag{36}$$

if $\eta=0$ and

$$u_n = \frac{b(1-q^2)^2}{(1-bq^2)(b-q^2)}\left[q^{2n-1} - \frac{q(1-bq^2)+b(bq+q+1+q^2)}{(b+1)(1+q)}b^{-n}\right]G\cos k. \tag{37}$$

if $\eta=1$, where $n=1,2,\ldots$. Next, using in the same manner as above, the symmetry properties of the lattice fields φ_n and u_n given by Eqs. (18) as well as the expressions (35)–(37), we find that the energy functional (30) is transformed to

$$\frac{E_{B\nu}(b,\lambda_\nu;q)}{\cos k} = (1-q)^2 - \lambda_\nu \frac{(1-q^2)^3}{(b-q^2)^2} P_{B\nu}(b;q), \quad \nu=0,1, \tag{38}$$

where the explicit form of the functions $P_{B\nu}$ is also presented in Appendix B [see Eq. (B1)]. As above, these functions also tend to $b/2$ if $q\to 1$.

C. Energy surfaces and delocalized states

The four variational functions $E_{S\nu}(b,\lambda_\nu;q)$ and $E_{B\nu}(b,\lambda_\nu;q)$, $\nu=0,1$, given by Eqs. (34) and (38) are the basic results of the analytical approach developed in this paper. The two-dimensional plots of one of these functions, namely, $\Phi_0(q)\equiv E_{S0}(b,\lambda_0;q)/\cos k$, are presented in Figs. 1 and 2, which include the dependence on the parameters λ_0 and ζ, respectively.

Both these plots show that the minimum of the variational energy $\Phi_0(q)$ disappears, for sufficiently small coupling constant λ_0 at ζ fixed (see Fig. 1 and the curve on the surface), or sufficiently large ζ at λ_0 fixed (see Fig. 2). This is contrary to the limiting case $\zeta\to 1$, when there exists the continuous transition from the small polaron regime to the large one if the constant λ_0 tends to zero. In other words, the polaron regime for a sufficiently big parameter b or a sufficiently weak coupling constant λ_0, at certain critical values of these parameters, suddenly disappears.

Figure 3 shows details of the drastic behavior of the energy function $\Phi_0(q)$. Here, curve 1 represents the energy behavior of the system in the limiting case $\zeta=1$, when the on-site potential is absent. In this case there exists only one minimum in the interval $0<q<1$ that corresponds to the polaron solution being a ground state of the system. After we introduce an on-site potential ($\zeta>1$), the energy surface changes and another local minimum appears at $q=1$ (see curve 2 in the inset of Fig. 3).

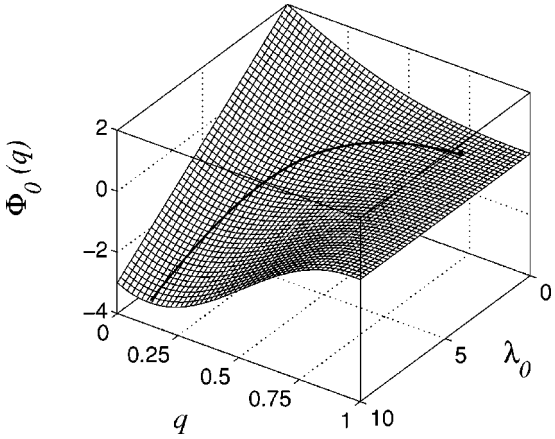

FIG. 1. Variational function $\Phi_0(q)$ plotted as a two-dimensional surface against q and λ_0 at the fixed value of the parameter $b(\zeta=1.25)$. The curve on this surface shows the set of minima of the function $\Phi_0(q,\lambda_0)$.

This minimum, at which the variational energy $\Phi_0(q)$ always equals zero [see Eq. (34)], corresponds to the extended, completely delocalized state. When we decrease λ_0 (at ζ fixed) or increase ζ (at λ_0 fixed), the size of the polaron profile increases and the energy minimum becomes more and more shallow. At a certain critical value of λ_0 or ζ, the variational energy at both the minima becomes the same (equal to zero) as demonstrated by curve 3 in Fig. 3. Further decrease of λ_0 or increase of ζ results in increasing the energy at the self-localized state that becomes positive, exceeding the zero energy of the delocalized state. Therefore, the polaron state becomes metastable, whereas the delocalized state becomes a ground state. This situation is illustrated by curve 4 in Fig. 3. Finally, with further decreasing λ_0 or increasing ζ, the polaron state disappears and only one minimum at $q=1$, which corresponds to the delocalized state, remains (see curve 5).

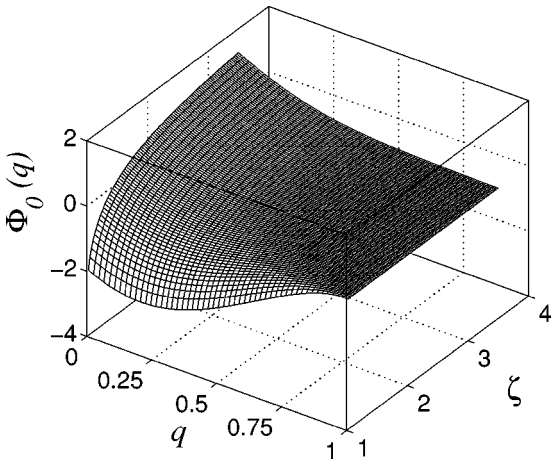

FIG. 2. Variational function $\Phi_0(q)$ plotted as a two-dimensional surface against q and ζ at the fixed value $\lambda_0=5$.

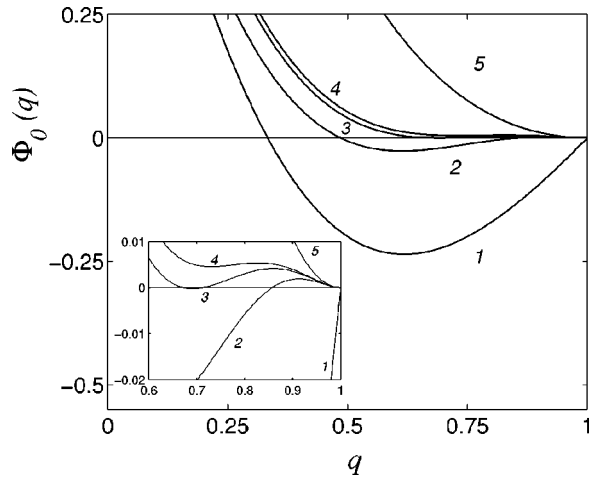

FIG. 3. Variational function $\Phi_0(\zeta,\lambda_0;q)$ against the parameter q for different values of the parameters ζ and λ_0: $\zeta=1$ and $\lambda_0=1$ (curve 1), $\zeta=1.3$ and $\lambda_0=2$ (curve 2), $\zeta=1.3875$ and $\lambda_0=2$ (curve 3), $\zeta=1.415$ and $\lambda_0=2$ (curve 4), and $\zeta=12.5$ and $\lambda_0=2$ (curve 5).

Thus, we have obtained three possible regimes: (i) the polaron is a ground state and the delocalized state is metastable, (ii) the polaron state is metastable and the delocalized state is a ground state, and (iii) the polaron does not exist and only the delocalized state is possible. A similar situation takes place in the other three cases described by the variational energies E_{S1}, E_{B0}, and E_{B1}.

Having found an optimal value of the variational parameter q for each set of the system parameters, one can plot a corresponding two-component polaron profile: the envelope φ_n [using Eqs. (31) and (35)] and the displacement field u_n [using Eqs. (32), (33), (36), and (37)]. Figure 4 demonstrates the site-centered polaron profiles for the case $\eta=0$ and two sets of the parameters that correspond to curves 2 and 3 in Fig. 3. The bond-centered polaron profile for the case $\eta=1$ is presented in Fig. 5.

V. A CRITERION FOR THE EXISTENCE OF SELF-LOCALIZED STATES

As demonstrated in the previous section, the variational functions $E_{S\nu}(b,\lambda_\nu;q)$ and $E_{B\nu}(b,\lambda_\nu;q)$, $\nu=0,1$, given by Eqs. (34), (38), and (B1), do not always admit minima that correspond to self-localized states. To analyze them, it is convenient to represent the equations for extrema $\partial E_{S\nu}/\partial q=0$ and $\partial E_{B\nu}/\partial q=0$ in the form

$$F(b;q)\equiv\frac{1-q^2}{(b-q^2)^3}W(b;q)=\frac{1}{\lambda}, \tag{39}$$

where the subscripts $S\nu$ and $B\nu$ have been omitted for a while. The explicit form of the functions $W(b;q)$ is given in Appendix B [see Eq. (B2)] and the constants λ (with subscript ν also omitted) are defined by Eqs. (A5) and (A10). Since each W is a weakly varying function that is bounded from above, it follows from Eq. (39) that for any $b>1$, there exist sufficiently small values of the parameter λ when Eq. (39) does not possess a solution. On the other hand, in the case without any on-site potential ($b=1$), the polaron solutions are known to exist for any constant $\lambda>0$. Indeed, in the limit $b\to1$, Eq. (39) becomes

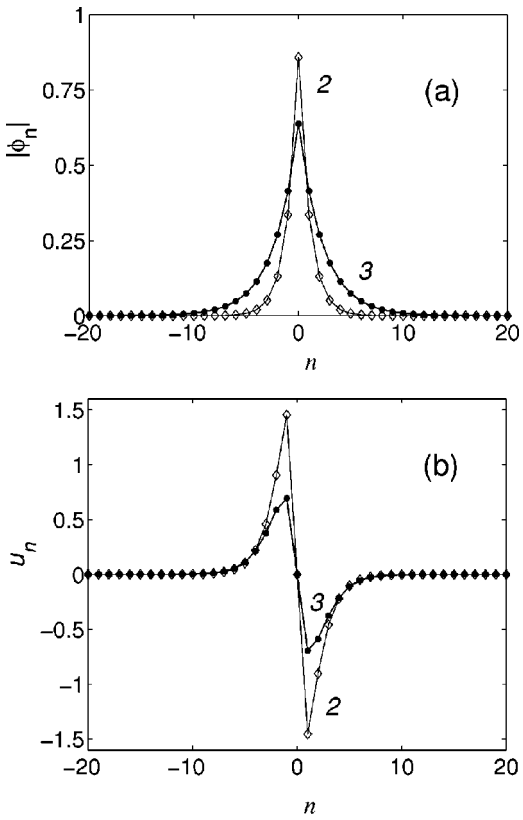

FIG. 4. Site-centered polaron profiles for $\eta=0$: (a) wavefunction envelope φ_n, and (b) displacement field u_n correspond to the minima of the variational function $\Phi_0(q)$ plotted as curves 2 and 3 in Fig. 3. The system parameters for curves 1 and 2 are the same as for curves 2 and 3 in Fig. 3, respectively.

$$\frac{q}{1-q}=\frac{Y(q)}{\lambda}, \tag{40}$$

with the function $Y(q)$ given explicitly in Appendix B for each particular case [see Eq. (B3)]. The left-hand side of Eq. (40) is a monotonically increasing function from zero to infinity and therefore, for any λ, this equation always admits a unique solution. This solution corresponds to the Davydov soliton in an isolated molecular chain.[1–3,7,20]

The situation changes drastically in the case $b>1$, when the left-hand side of Eq. (39) becomes a convex function that equals zero at $q=0$ and $q=1$. Let $q_m=q_m(b)$ be the point in the interval $0<q<1$ at which the function $F(b;q)$ attains a maximum. If the coupling constant λ is large enough, the line $1/\lambda$ will cross the curve $F(b;q)$ at two points, so that Eq. (39) will have two roots corresponding to extrema of the variational energy. The smaller root corresponds to a (polaron) minimum of the energy, while the bigger root corresponds to a maximum of this energy that separates the polaron minimum and the minimum at $q=1$ responsible for the delocalized state.

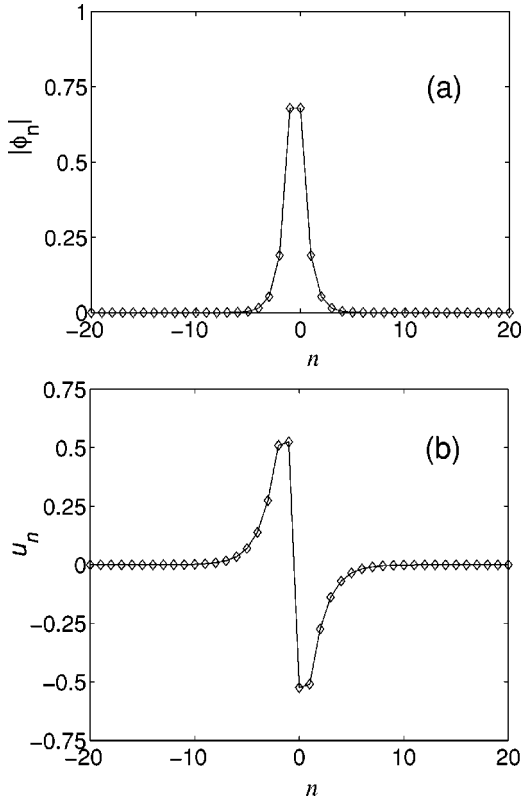

FIG. 5. Bond-centered polaron profiles for $\eta=1$, $\zeta=1.25$, and $\lambda_1=4$: (a) wave-function envelope φ_n, and (b) displacement field u_n components.

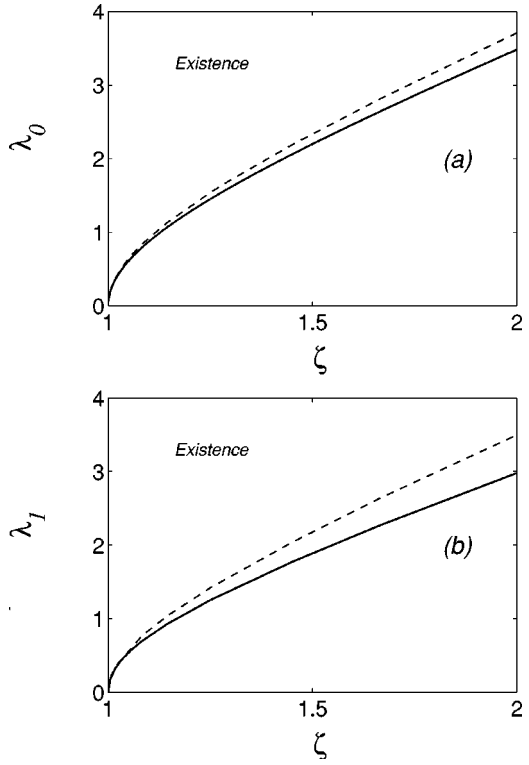

FIG. 6. Diagrams of existence of site-centered polaron states for (a) $\eta=0$, and (b) $\eta=1$. Solid curves separate the regions of existence and nonexistence of polaron solutions, while dashed curves separate stable and metastable polaron solutions.

With decreasing λ, these two extremal points move towards each other and eventually merge at some critical value of λ. With further decrease of λ, the polaron solution disappears completely. We denote $\mathcal{B}(b)\equiv\max_q F(b;q)=F[b;q_m(b)]$. Then the condition for the existence of polaron solutions, i.e., roots of Eq. (39), is the inequality

$$\mathcal{B}(b)\lambda>1. \tag{41}$$

Therefore, the (b,λ) plane can be split into two regions by the line $\mathcal{B}(b)\lambda=1$. This line separates the regions of existence and nonexistence of self-localized states.

To be more precise, we consider first the site-centered solutions with $\eta=0$ and fix the value $b=2$. In this case, the function $F(2;q)$ has a maximum at the point $q_m=\sqrt{2/3}$. Inserting this value for q_m into the equation $F(2;q_m)=\lambda_0^{-1}$, we find the critical value of λ_0 at which the self-trapping appears. The self-trapped state exists for all $\lambda_0>4(2/3)^{5/2}$.

In the general case, with any $b>1$, differentiating the function $F(b;q)$ with respect to q, equating the resulting expression to zero, and solving the resulting equation, we find the value q_m in the interval $0<q<1$ at which the function $F(b;q)$ reaches a maximum:

$$q_m^2=\frac{5b^2-8b+5-(b-1)\sqrt{25b^2-22b+25}}{2(2-b)}. \tag{42}$$

This expression is well defined for all $b>1$, including the particular case $b=2$ mentioned above, as well as the limit $b\to\infty$ for which $\lim_{b\to\infty}q_m^2=2/5$. In Fig. 6(a) we have plotted the line $\lambda_0=\mathcal{B}_{S0}^{-1}(b)=F[b;q_m(b)]^{-1}$ as a solid curve. This curve separates the regions of existence and nonexistence of polaron states. The dashed line, calculated by comparing the energy (34) in different polaron states with the zero energy (at $q=1$), separates stable and metastable polaron states. Similar diagrams of the existence of site-centered self-localized solutions have been plotted in Fig. 6(b) for the case $\eta=1$. In this case, there are no analytical solutions like Eq. (42) and therefore both the solid and dashed lines, with the same meaning as in Fig. 6(a), were calculated numerically, using Eqs. (34), (39), and (41).

VI. BINDING ENERGY OF THE SELF-LOCALIZED (QUASI)PARTICLE

The dimensionless binding energy of the (quasi)particle ε, which can be calculated according to Eq. (12), is the lowest energy level of the Schrödinger equation (8). Using the envelope φ_n and the displacement field u_n given by Eqs. (31)–(33) and (35)–(37) as well as the definitions (A5) and (A10), this energy can be expressed through the variational parameter q. The resulting equations are

$$\frac{\varepsilon}{\cos k}=2\frac{(1-q)^2}{1+q^2}-2\lambda_\nu\frac{(1-q^2)^3}{(b-q^2)^2}P_{S\nu}(b;q),\quad \nu=0,1, \tag{43}$$

for the S self-trapped states and

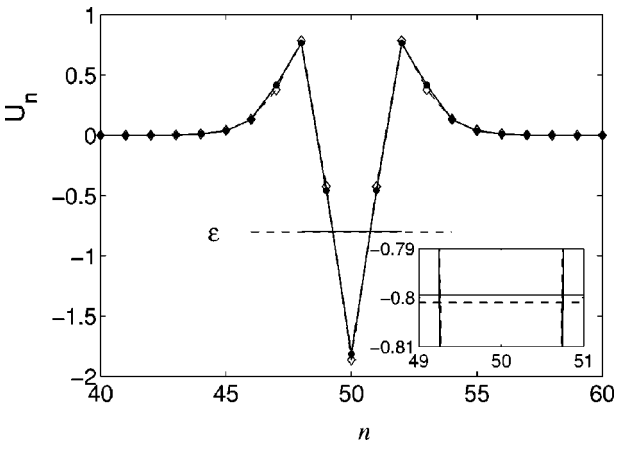

FIG. 7. Effective deformation potential U_n and the lowest energy level ε calculated numerically (solid lines) and analytically (dashed lines) for $\eta=0$ ($\alpha=4$, $\beta=5$, $\lambda_0=5$, and $\zeta=2$). The inset shows an enlargement of the binding level.

$$\frac{\varepsilon}{\cos k}=(1-q)^2-2\lambda_\nu\frac{(1-q^2)^3}{(b-q^2)^2}P_{B\nu}(b;q),\quad \nu=0,1, \tag{44}$$

for the B self-trapped states.

In the particular case $\eta=0$ and $k=0$, the discrete Schrödinger equation (8) can be rewritten in the form

$$-(\varphi_{n+1}-2\varphi_n+\varphi_{n-1})+U_n\varphi_n=\varepsilon\varphi_n, \tag{45}$$

where $U_n=\alpha(u_{n+1}-u_{n-1})/2$ is the deformation potential formed in the chain by a (quasi)particle (an excitation or an electron). The energy level ε and the potential U_n were calculated by minimization of the discrete energy functional (30), resulting in a numerically exact polaron solution, and then inserting this solution into Eq. (12). The results of these numerical calculations have confirmed the analytical results given by Eqs. (32), (33), (36), (37), (43), and (44) to very high accuracy. Figure 7 illustrates, for the case $\eta=0$, the comparison of the variational approximation given by the trial function (31) with the corresponding numerically exact polaron solution found by minimization of the energy (30).

VII. PINNING AND MOBILITY OF POLARONS

In general, while propagating along the chain, a narrow polaron (or another solitary wave, except for the supersonic pulse soliton in the Fermi-Pasta-Ulam type chain) radiates small-amplitude waves, and finally stops because of a so-called Peierls-Nabarro (PN) periodic potential relief. The existence of such a relief (barrier) is an effect of lattice discreteness.[29] In this section, we extend the studies of the PN barrier for the Davydov soliton, carried out previously[30] for the case of an isolated molecular chain, to the case with an on-site potential ($b>1$).

According to Eqs. (34) and (38), we have calculated the polaron energy in the S and B states for $\eta=0$ and $\eta=1$. Particularly, for the case $\eta=0$ with $b=1$ at $k=0$ and for the same system parameters, the energy in the S state given by Eq. (34) appeared to be lower than that in the B state, which is given by Eq. (38). This result coincides with that found previously,[30] i.e., the site-centered profile corresponds to a minimum of the polaron energy, whereas the bond-centered profile is associated with a saddle point. Surprisingly, similar calculations of the energies (34) and (38) for the case $\eta=1$ gave the opposite energy inequality hold: the B self-localized state was found to have lower energy than the S state. Thus, for standing ($k=0$) self-localized states the following two inequalities: $E_{S0}<E_{B0}$ and $E_{B1}<E_{S1}$. Therefore, one can expect that for a certain intermediate value $\eta=\eta_c$, the barrier defined by the difference $\Delta E=\Delta(\eta)\equiv|E_B(\eta)-E_S(\eta)|$ will disappear, so that the equality $\Delta E(\eta_c)=0$ should be valid. For this purpose, we have calculated numerically the height of this barrier as a function of η, minimizing the energy functional (30). The dependencies $\Delta E=\Delta E(\eta)$ (solid line) and $E_B(\eta)-E_S(\eta)$ (dashed line) for $\lambda=5$ [see Eq. (16), $k=0$] and $\zeta=2$ are shown in Fig. 8 that demonstrate the existence of a critical value η_c at which the $\Delta E=0$ barrier entirely disappears.

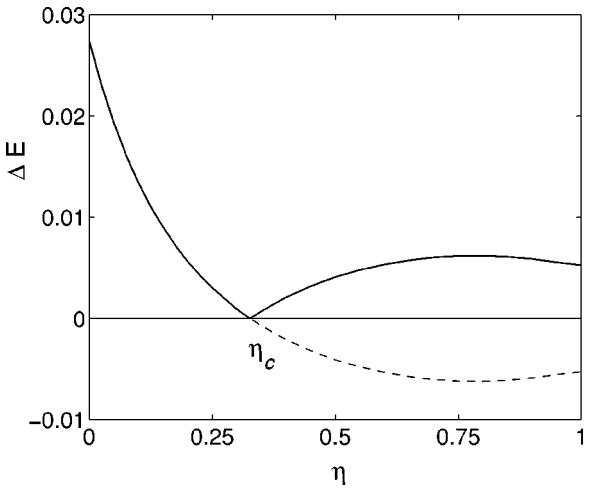

FIG. 8. Height of the pinning barrier ΔE (solid line) and the energy difference E_B-E_S (dashed line) as functions of the parameter η for $\lambda=5$ and $\zeta=2$.

We have calculated this critical value for different system parameters. These results are presented in Table I.

They show that the critical value η_c depends very weakly on the system parameters and remains within the interval 0.32–0.35. Increase of the coupling constant $\lambda=\alpha\beta/4$ or decrease of the on-site parameter κ_0 causes insignificant shift of η_c towards higher values. Note that ΔE is not PN barrier, but just its estimate from below.

Such a behavior of the pinning barrier gives us a reason to expect that a movable polaron can exist that does not expe-

TABLE I. Dependence of the critical value η_c on the strength of the on-site potential κ_0 and the coupling parameter λ.

λ	$\kappa_0=0.25$	$\kappa_0=0.5$	$\kappa_0=1$	$\kappa_0=2$	$\kappa_0=3$
2	0.3339	0.3316			
5	0.3385	0.3357	0.3315	0.3266	0.3229
10	0.3429	0.3395	0.3355	0.3295	0.3260

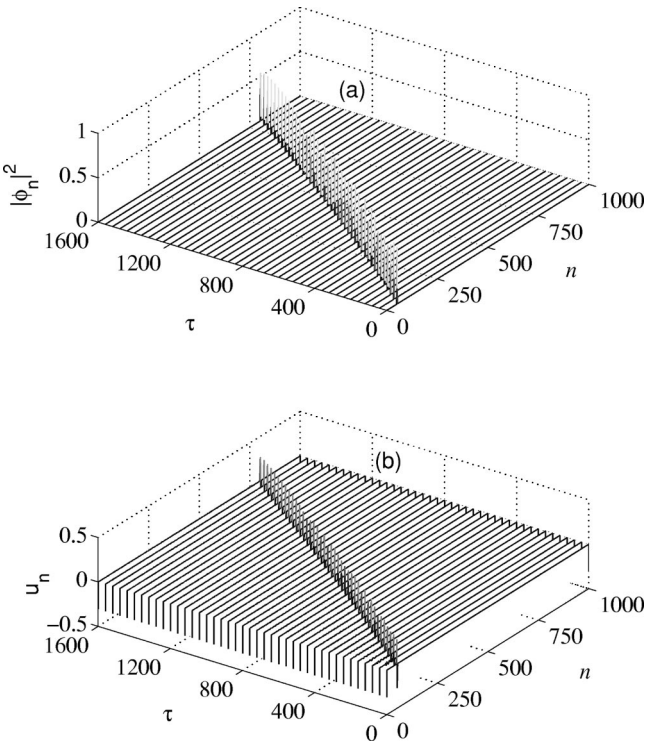

FIG. 9. Dynamics of lattice fields (a) $|\phi_n(\tau)|^2$, and (b) $u_n(\tau)$, in the chain consisting of $N=1000$ particles ($\alpha=10$, $\beta=4$, $\zeta=2.5$, $\sigma=1$, and $\eta=\eta_c=0.325\,965$).

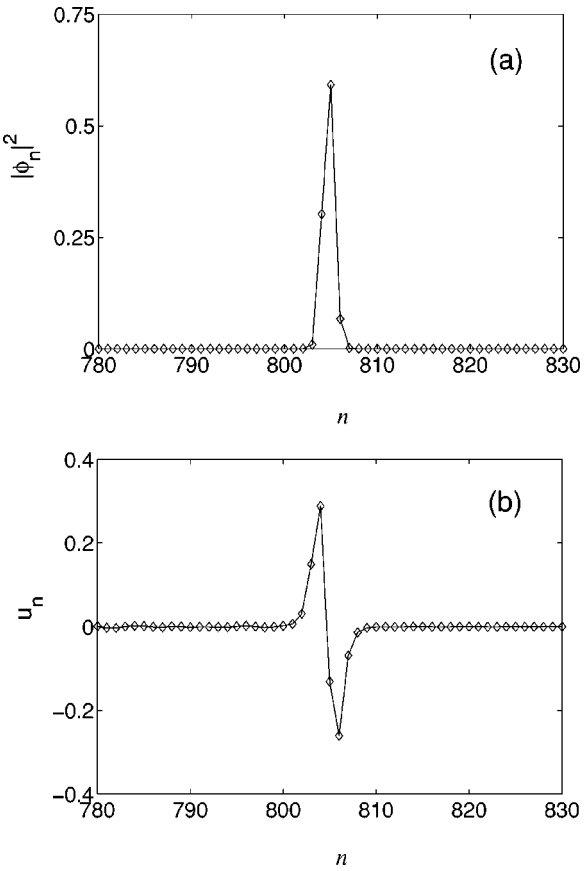

FIG. 10. Final polaron profiles of lattice fields (a) $|\phi_n(\tau_f)|^2$, and (b) $u_n(\tau_f)$, at final time instant $\tau=\tau_f=1600$, the dynamics of which is displayed in Fig. 9.

rience any lattice effects. In order to check this, we simulated equations of motion (5) and (6) for the critical value $\eta_c=0.325\,965$, using the fourth order Runge-Kutta scheme with the time step $\Delta\tau=0.02$. This case should correspond to the transparent polaron motion through the chain, despite the fact that the parameter values were chosen to form a quite narrow polaron profile. Therefore we have substituted the polaron solution obtained before by minimization of the functional (30) into the basic equations of motion (5) and (6) reduced to the corresponding dimensionless form through the scaled wave function $\phi_n(\tau)$ and displacement field $u_n(\tau)$. The initial conditions were chosen according to the relations $du_n/d\tau \simeq -s(u_{n+1}-u_n)$ and $\phi_n(0)=\varphi_n\exp(ikn)$, where φ_n and u_n represent the polaron solution found by minimization of the energy (30). Here we have approximately replaced the time derivative by the spatial derivative. This is, of course, a very crude approximation for narrow polaron profiles, but it gives a proper initial kick to the polaron. We have chosen the wavevector $k=0.4$ that corresponds to the velocity $s=2\sigma\sin k\simeq 0.78$. The results of simulations are presented in Fig. 9.

Initially, right after the initial kick, the polaron emits some radiation and slows down, but later it separates itself from the radiation and propagates with constant velocity that is quite close to $s=0.78$. The final snapshot of the polaron profile is presented in Fig. 10. As can be seen in these plots, the profile appears to be very narrow, propagating without significant energy loss. Some tiny radiation can be explained by very crude approximation of the initial conditions.

In order to emphasize the depinning effect, we performed similar simulations for η slightly different from the critical value. We took $\eta=0.24$, while the rest of the system parameters were kept unchanged, and created the initial conditions in the same way as before. In this case, the polaron did not manage to move further than 12 chain sites and eventually got pinned. The results of these simulations are presented in Fig. 11.

VIII. CONCLUSIONS

Contrary to the one-dimensional acoustic polaron (Davydov-Scott) theory,[1,2] where the self-trapping occurs for all values of the system parameters, we have shown in this paper that the presence of a physically reasonable external on-site potential for each chain molecule leads in some cases to the nonexistence of self-localized (polaron) states. It happens that for some parameter values the self-trapping exists, while for other values only delocalized states are possible. We have found the criterion for the existence of self-localized states given by the inequality (41). In particular, for the existence of polaron states the (quasi)particle-lattice coupling constant χ_1 or χ_2 should be sufficiently large or the strength κ_0 of the on-site potential should be sufficiently weak. This criterion is also valid for narrow polaron solutions which are immobile, so that even for standing one-dimensional polarons, their formation depends on the system parameters.

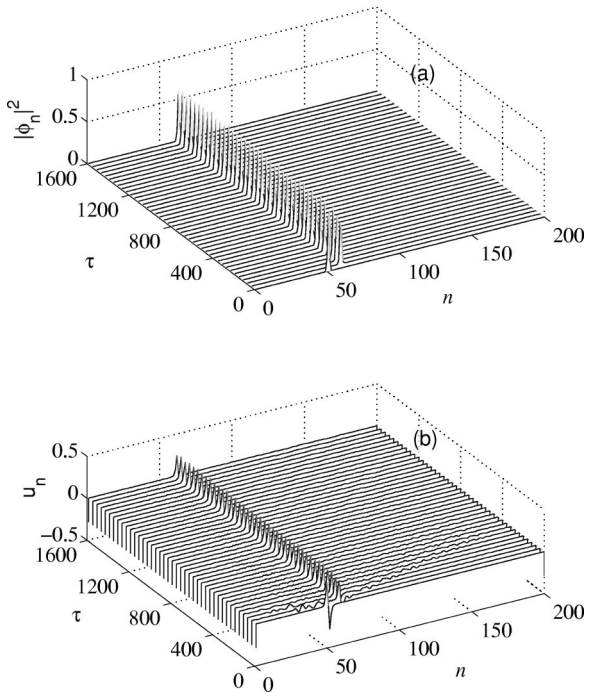

FIG. 11. Dynamics of lattice fields (a) $|\phi_n(\tau)|^2$ and (b) $u_n(\tau)$ in the chain with $N=1000$ particles ($\alpha=10$, $\beta=4$, $\zeta=2.5$, $\sigma=1$, and $\eta=0.24$).

It is important to note that the delocalized (exciton) state does always exist in the chain, being therefore in some cases stable (a ground state) and in other cases metastable. More precisely, the following three regimes (three types of solutions) can exist in the chain with an on-site potential: (i) the polaron as a ground state and the exciton as a metastable state, (ii) the polaron as a metastable state and the exciton as a (delocalized) ground state, and (iii) the polaron state does not exist and only the exciton is a ground state. The analytical calculations performed in this paper allow us to investigate the physical mechanisms of the existence and nonexistence of the self-trapping and to find two characteristic parameters b and λ, in terms of which we were able to formulate the criterion of the polaron existence [see Eq. (41)]. In the simplest case when the polaron is standing and $\chi_2=0$, these parameters are $b=1+\kappa_0/2K+\sqrt{\kappa_0/K+(\kappa_0/2K)^2}$ and $\lambda=\chi^2 l^2/JK$. For moving polarons, the ratio κ_0/K and the reduced coupling constant λ are renormalized accordingly. If the on-site potential is sufficiently strong or the (quasi)particle-phonon coupling is sufficiently weak, the chain particles prefer to stay in the well of the on-site potential and the exciton-phonon interaction cannot displace them from the potential minima to support a stationary traveling-wave motion along the chain of a self-localized state. As illustrated by Fig. 3, the existence of both self-localized and delocalized solutions results in the appearance of an effective barrier that separates these states.

Although analytical calculations and techniques appear to be very lengthy and complicated, the final results presented by the variational functions (34) and (38) seem to be simple and these are the main findings of the present paper. We have introduced a whole variety of series that we call hyperbolic Chebyshev polynomials. This approach can be applied to other models of the polaron theory.

Surprisingly, it was found that stable self-localized states appear to occur with different (on-site or on-bond) symmetry. This is due to the different physical meaning of the coupling constants χ_1 and χ_2 mentioned in the Introduction. This result prompted us to seek the ratio of these constants when depinning of a polaron occurs. We have found that it happens at the value $\eta=\chi_2/(\chi_1+\chi_2)\simeq 0.33$ and confirmed by simulations that the polaron in the chain with this ratio can propagate freely, similarly to transparent propagation of narrow topological defects in discrete nonlinear Klein-Gordon systems.[31]

ACKNOWLEDGMENTS

Y.Z. wishes to acknowledge the financial support from Heriot-Watt University and the Max-Planck-Institut für Physik Komplexer Systeme. We are also grateful for support under the LOCNET EU network HPRN-CT-1999-00163. Useful discussions with S. Aubry are also acknowledged.

APPENDIX A: DISPLACEMENT FIELDS AND CORRESPONDING DNLS EQUATIONS

1. Site-centered self-localized states

a. The case $\eta=0$ ($\chi_1>0$, $\chi_2=0$)

Using Eq. (15) for the particular case $\eta=0$, the result Eq. (25) can be rewritten in terms of φ_j^2, $j=0,1,\ldots$, as follows:

$$u_1=G\left[-(b^{-1}\varphi_0^2+b^{-2}\varphi_1^2)+(b-b^{-1})\sum_{j=2}^{\infty} b^{-j}\varphi_j^2\right]. \tag{A1}$$

In this series, the first two terms are negative while the others are positive. Substituting the series (A1) in Eq. (19) where R_j is defined by Eq. (15) with $\eta=0$ and using the representation for the polynomials $K_n^{[2\zeta]}$ given by Eq. (24), we find the following series for the displacement u_n:

$$u_n=G\sum_{j=0}^{\infty} A_{jn}\varphi_j^2, \quad n\geqslant 1, \tag{A2}$$

where the matrix coefficients A_{jn}, $j=0,1,\ldots$, $n=1,2,\ldots$, are given by

$$A_{0n}=-b^{-n}, \quad n\geqslant 1,$$

$$A_{jn}=-(b^j+b^{-j})b^{-n}, \quad 1\leqslant j\leqslant n-1, \quad n\geqslant 2,$$

$$A_{nn}=-b^{-2n}, \quad n\geqslant 1,$$

$$A_{jn}=b^{-j}(b^n-b^{-n}), \quad j\geqslant n+1, \quad n\geqslant 1. \tag{A3}$$

Using the series representation (A2) in Eq. (8) with $\eta=0$, we get the following stationary DNLS equation:

$$\varphi_{n+1}-2\varphi_n+\varphi_{n-1}+\lambda_0\sum_{j=0}^{\infty}(A_{j,n-1}-A_{j,n+1})\varphi_j^2\varphi_n$$
$$+(\varepsilon/\cos k)\varphi_n=0,\quad n\geqslant 0, \tag{A4}$$

where $A_{j0}=0$, $A_{j,-1}=A_{j1}$, and $\varphi_{-1}=\varphi_1$. Here the (quasi)particle-phonon coupling parameter λ_0 is given through the expression for λ defined by Eq. (16):

$$\lambda_0\equiv\lambda\big|_{\eta=0}=\alpha\beta/4(1-s^2)\cos k. \tag{A5}$$

b. The case $\eta=1$ ($\chi_1=0$, $\chi_2>0$)

Similarly, using the expression (15) at $\eta=1$, the series (25) is rewritten in terms of $\varphi_j\varphi_{j+1}$, $j=0,1,\ldots,$ as follows:

$$u_1=2G\cos k\left[-b^{-1}\varphi_0\varphi_1+(1-b^{-1})\sum_{j=1}^{\infty}b^{-j}\varphi_j\varphi_{j+1}\right]. \tag{A6}$$

Here the first term is negative while the others are positive. In the same way as above, using Eq. (15) with $\eta=1$, the explicit formula (24), and the series (A6), we find that the series (19) is transformed to

$$u_n=2G\cos k\sum_{j=0}^{\infty}B_{jn}\varphi_j\varphi_{j+1},\quad n\geqslant 1, \tag{A7}$$

where the coefficients B_{jn}, $j=0,1,\ldots,$ $n=1,2,\ldots,$ are given by

$$B_{0n}=-b^{-n},\quad n\geqslant 1,$$
$$B_{jn}=-\frac{1}{b+1}(b^{j+1}+b^{-j})b^{-n},\quad 1\leqslant j\leqslant n-1,\quad n\geqslant 2,$$
$$B_{jn}=\frac{1}{b+1}b^{-j}(b^n-b^{-n}),\quad j\geqslant n\geqslant 1. \tag{A8}$$

In a similar way, using the series (A7), Eq. (8) at $\eta=1$ is transformed to

$$\varphi_{n+1}-2\varphi_n+\varphi_{n-1}+2\lambda_1\sum_{j=0}^{\infty}[(B_{j,n-1}-B_{jn})\varphi_{n-1}+(B_{jn}$$
$$-B_{j,n+1})\varphi_{n+1}]\varphi_j\varphi_{j+1}+(\varepsilon/\cos k)\varphi_n=0,\quad n\geqslant 0, \tag{A9}$$

where $B_{j0}=0$, $B_{j,-1}=-B_{j1}$, and $\varphi_{-1}=\varphi_1$. The reduced coupling parameter λ_1 is given by [see Eq. (16)]

$$\lambda_1\equiv\lambda\big|_{\eta=1}=\alpha\beta\cos k/4(1-s^2). \tag{A10}$$

2. Bond-centered self-localized states

a. The case $\eta=0$ ($\chi_1>0$, $\chi_2=0$)

In the same way as for the *S* states, using Eq. (15) for the particular case $\eta=0$, the series (29) can be rewritten in terms of φ_j^2, $j=1,2,\ldots,$ as follows:

$$u_1=G\left[-b^{-1}\varphi_1^2+(b-1)\sum_{j=2}^{\infty}b^{-j}\varphi_j^2\right], \tag{A11}$$

where we have used the relation $\varphi_0=\varphi_1$ [see Eq. (18)]. The first term of the series (A11) is negative while the others are positive. Substituting next the series (A11) in Eq. (26), where R_j is defined by Eq. (15) with $\eta=0$ and using the representation for the polynomials $K_n^{[2\zeta]}$ and $K_n^{[2\zeta+1]}$ given by Eqs. (24) and (28), we find the displacement field u_n as a series

$$u_n=G\sum_{j=1}^{\infty}C_{jn}\varphi_j^2,\quad n\geqslant 1, \tag{A12}$$

where the matrix coefficients C_{jn}, $j,n=1,2,\ldots,$ are given by

$$C_{nn}=-b^{-2n+1},\quad n\geqslant 1,$$
$$C_{jn}=-(b^j+b^{-j+1})b^{-n},\quad 1\leqslant j\leqslant n-1,\quad n\geqslant 2,$$
$$C_{jn}=b^{-j}(b^n-b^{-n+1}),\quad j\geqslant n+1,\quad n\geqslant 1. \tag{A13}$$

Similarly, using the series representation (A12) in Eq. (8) with $\eta=0$, one obtains the stationary DNLS equation

$$\varphi_{n+1}-2\varphi_n+\varphi_{n-1}+\lambda_0\sum_{j=1}^{\infty}(C_{j,n-1}-C_{j,n+1})\varphi_j^2\varphi_n$$
$$+(\varepsilon/\cos k)\varphi_n=0,\quad n\geqslant 1, \tag{A14}$$

where $C_{j0}=-C_{j1}$, $\varphi_0=\varphi_1$, and the coupling constant λ_0 is given by Eq. (A5).

b. The case $\eta=1$ ($\chi_1=0$, $\chi_2>0$)

In the same way as for the *S* states, using the expression (15) at $\eta=1$, the series (29) is rewritten in terms of $\varphi_j\varphi_{j+1}$, $j=0,1,\ldots,$ as

$$u_1=\frac{2G\cos k}{b+1}\left[-\varphi_1^2+(b-1)\sum_{j=1}^{\infty}b^{-j}\varphi_j\varphi_{j+1}\right]. \tag{A15}$$

As above, the first term in this series is negative while the others are positive. Using next Eq. (15) with $\eta=1$, and inserting the expressions (24), (28), and (A15) in the series (26), we find

$$u_n=2G\cos k\sum_{j=0}^{\infty}D_{jn}\varphi_j\varphi_{j+1},\quad n\geqslant 1, \tag{A16}$$

where $\varphi_0=\varphi_1$ and the coefficients D_{jn}, $j=0,1,\ldots,$ $n=1,2,\ldots,$ are given by

$$D_{0n}=-\frac{b^{-n+1}}{b+1},\quad n\geqslant 1,$$
$$D_{jn}=-\frac{1}{b+1}(b^j+b^{-j})b^{-n+1},\quad 1\leqslant j\leqslant n-1,\quad n\geqslant 2,$$

$$D_{jn}=\frac{1}{b+1}b^{-j}(b^n-b^{-n+1}),\quad j\geqslant n,\quad n\geqslant 1. \quad \text{(A17)}$$

Similarly, the corresponding DNLS equation is found from Eq. (8) with $\eta=1$, using the representation (A16):

$$\varphi_{n+1}-2\varphi_n+\varphi_{n-1}+2\lambda_1\sum_{j=0}^{\infty}[(D_{j,n-1}-D_{jn})\varphi_{n-1}+(D_{jn}-D_{j,n+1})\varphi_{n+1}]\varphi_j\varphi_{j+1}+(\varepsilon/\cos k)\varphi_n=0,\quad n\geqslant 1, \quad \text{(A18)}$$

where $D_{j0}=-D_{j1}$, $\varphi_0=\varphi_1$, and the coupling constant λ_1 is given by Eq. (A10).

The nonlinearity in each of the stationary DNLS equations (A4), (A9), (A14), or (A18) contains infinite series that in the continuum limit are transformed to integral terms. It can easily be checked that in the limiting case $b\to 1$ the coefficients (A3), (A8), (A13), and (A17) take a simple form, so that the series in the corresponding DNLS equations are reduced to single cubic nonlinear terms.

APPENDIX B: THE *P*, *W*, AND *Y* FUNCTIONS AND THEIR BEHAVIOR

The four functions $P(b;q)$ that appear in Eqs. (34) and (38) are given by

$$P_{S0}=\frac{b}{1+q^2},\quad P_{S1}=\frac{4bq^2}{(1+q^2)^3},\quad P_{B0}=\frac{1}{4}(2b+1-q^2),$$

$$P_{B1}=\frac{(1-q)[(2b+q)q(1+q^2)+b(b+q^2)]+2bq^2(b+q)}{(b+1)(1+q)(1+q^2)}. \quad \text{(B1)}$$

The functions (B1) have small variation in the interval $0\leqslant q\leqslant 1$ and each of them tends to $b/2$ if $q\to 1$.

The other four functions $W(b;q)$ that are involved in Eq. (39) as factors have also small variation and are given explicitly by

$$W_{S0}=bq(2b-1+bq^2-2q^2),$$

$$W_{S1}=\frac{2bq}{(1+q^2)^2}(-b+6bq^2-q^2+bq^4-6q^4+q^6),$$

$$W_{B0}=\frac{1}{2}q(1+q)(3b^2-1-3bq^2+q^4),$$

$$W_{B1}=\frac{1}{(b+1)(1+q^2)^2}\{(b-1)[b^2(1+q-q^2+8q^3-q^4+5q^5)+bq(1+q+6q^2+14q^3-9q^4+7q^5-8q^6)+q^3(7+6q-3q^2-8q^3-6q^5+3q^6)]+2q^3(1-q^2)\times(1+q)(3-q^4)\}. \quad \text{(B2)}$$

In each of the four cases $S\nu$ and $B\nu$, $\nu=1,2$, the functions $Y(q)$ [see Eq. (40)] are defined by

$$Y_{S0}=1+q,\quad Y_{S1}=\frac{(1+q)(1+q^2)^2}{2(4q^2-1-q^4)},$$

$$Y_{B0}=\frac{2}{2-q^2},\quad Y_{B1}=\frac{(1+q^2)^2}{q^2(3-q^4)}. \quad \text{(B3)}$$

All these four functions have the same limit ($Y\to 2$) when $q\to 1$.

[1] A. S. Davydov, *Solitons in Molecular Systems* (Reidel, Dordrecht, 1991).
[2] A. C. Scott, Phys. Rep. **217**, 1 (1992).
[3] L. Cruzeiro-Hansson and S. Takeno, Phys. Rev. E **56**, 894 (1997).
[4] Y. Zhao, D. W. Brown, and K. Lindenberg, J. Chem. Phys. **106**, 2728 (1997); **106**, 5622 (1997); **107**, 3159 (1997); D. W. Brown, K. Lindenberg, and Y. Zhao, *ibid.* **107**, 3179 (1997).
[5] P. E. Kornilovitch and E. R. Pike, Phys. Rev. B **55**, 8634 (1997); P. E. Kornilovitch, Phys. Rev. Lett. **81**, 5382 (1998); A. S. Alexandrov and P. E. Kornilovitch, *ibid.* **82**, 807 (1999); P. E. Kornilovitch, Phys. Rev. B **59**, 13 531 (1999).
[6] R. Roncaglia and G. P. Tsironis, Physica D **113**, 318 (1998).
[7] A. M. Clogston, H. K. McDowell, P. Tsai, and J. Hanssen, Phys. Rev. E **58**, 6407 (1998).
[8] S. Flach and K. Kladko, Phys. Rev. B **53**, 11 531 (1996).
[9] Y. Zolotaryuk and J. C. Eilbeck, J. Phys.: Condens. Matter **10**, 4553 (1998).
[10] D. Hennig, Phys. Rev. E **62**, 2846 (2000).
[11] E. Jeckelmann and S. R. White, Phys. Rev. B **57**, 6376 (1998); C. Zhang, E. Jeckelmann, and S. R. White, *ibid.* **60**, 14 092 (1999).
[12] A. H. Romero, D. W. Brown, and K. Lindenberg, J. Chem. Phys. **109**, 6540 (1998); Phys. Lett. A **254**, 287 (1999); Phys. Rev. B **59**, 13 728 (1999).
[13] G. Kalosakas, S. Aubry, and G. P. Tsironis, Phys. Rev. B **58**, 3094 (1998); Phys. Lett. A **247**, 413 (1998).
[14] L. Proville and S. Aubry, Physica D **113**, 307 (1998); Eur. Phys. J. B **11**, 41 (1999).
[15] D. Bambusi, J. Math. Phys. **40**, 3710 (1999).
[16] S. Raghavan, A. R. Bishop, and V. M. Kenkre, Phys. Rev. B **59**, 9929 (1999).
[17] L. Cruzeiro-Hansson, J. C. Eilbeck, J. L. Marín, and F. M. Russell, Phys. Lett. A **266**, 160 (2000).
[18] A. S. Davydov and N. I. Kislukha, Phys. Status Solidi B **59**, 465 (1973).
[19] S. Takeno, Prog. Theor. Phys. **71**, 395 (1984); **75**, 1 (1986).
[20] A. C. Scott, Phys. Rev. A **26**, 578 (1982).
[21] T. Holstein, Ann. Phys. (N.Y.) **8**, 325 (1959); **8**, 343 (1959).
[22] G. Careri, U. Buontempo, F. Carta, E. Gratton, and A. C. Scott,

Phys. Rev. Lett. **51**, 304 (1983); G. Careri, U. Buontempo, F. Galluzzi, A. C. Scott, E. Gratton, and E. Shyamsunder, Phys. Rev. B **30**, 4689 (1984).

[23] J. C. Eilbeck, P. S. Lomdahl, and A. C. Scott, Phys. Rev. B **30**, 4703 (1984); Physica D **16**, 318 (1985).

[24] A. V. Zolotaryuk, St. Pnevmatikos, and A. V. Savin, in *Davydov's Soliton Revisited*, edited by P. L. Christiansen and A. C. Scott (Plenum, New York, 1990), pp. 181–194; V. N. Kadantsev, L. N. Lupichev, and A. V. Savin, in *Nonlinear Phenomena in Extended Systems*, edited by L. N. Lupichev (Institute for Problems of Physics and Technology, Moscow, 1994), pp. 3–24.

[25] Y. Zolotaryuk, Ph.D. thesis, Heriot-Watt University, Edinburgh, 1998.

[26] A. V. Zolotaryuk, K. H. Spatschek, and O. Kluth, Phys. Rev. B **47**, 7827 (1993).

[27] W. C. Kerr and P. S. Lomdahl, Phys. Rev. B **35**, 3629 (1987).

[28] L. Fox and I. B. Parker, *Chebychev Polynomials in Numerical Analysis* (Oxford University Press, Oxford, 1968).

[29] M. Peyrard and M. D. Kruskal, Physica D **14**, 88 (1984).

[30] V. A. Kuprievich, Physica D **14**, 395 (1985); A. A. Vakhnenko and Yu. B. Gaididei, Teor. Mat. Fiz. **68**, 350 (1986) [Theor. Math. Phys. **68**, 873 (1987)].

[31] A. V. Savin, Y. Zolotaryuk, and J. C. Eilbeck, Physica D **138**, 267 (2000).